PCCP

Nanocomposites of colloidal gold particles and fatty acids formed by the high-affinity biotin–avidin interaction

Neeta Lala and Murali Sastry*

Materials Chemistry Division, National Chemical Laboratory, Pune–411 008, India.
E-mail: sastry@ems.ncl.res.in

Received 6th January 2000, Accepted 28th March 2000

The formation of thin nanocomposite films comprising colloidal gold particles in a fatty acid matrix by a simple solution based diffusion process is described. A simple two-step process accomplishes the formation of the composite films. In the first stage, avidin molecules are incorporated into thermally evaporated arachidic acid (AA) films by simple immersion of the lipid films in an aqueous solution of the protein. The diffusion of the avidin molecules is driven by attractive electrostatic interaction between charged side chains of the protein and the carboxylate ions of the AA matrix. Thereafter, biotinylated colloidal gold particles are incorporated into the protein-containing AA matrix by a similar immersion procedure. The high-affinity biotin–avidin interaction drives the diffusion of the biotinylated gold particles into the matrix and a colloidal nanocomposite results. The kinetics of protein incorporation as well as colloidal particle diffusion in the fatty acid matrix were characterized using quartz crystal microgravimetry (QCM) and ultraviolet–visible spectroscopy and analyzed in terms of a one-dimensional diffusion model. The nanocomposite films were further characterized by Fourier transform infrared (FTIR) spectroscopy which, together with the QCM and UV-vis spectroscopy measurements of the biotin–avidin recognition driven gold particle diffusion, indicates that the protein molecules are encapsulated in the fatty acid matrix without significant perturbation to their biological activity.

Introduction

The synthesis and organization of nanoscale inorganic materials is a problem of topical interest. Thin nanoparticle films of metals and semiconductors have been formed by a number of techniques. Some of the more prominent methods based on the use of colloidal nanoparticles include simple solution casting,[1,2] immobilization at the surface of self-assembled monolayers,[3,4] and organization at the air/water[5–7] and hydrosol/organic solution interfaces.[8] Thin films of metal and semiconductor nanoparticles have also been grown by chemical treatment of fatty acid salt Langmuir–Blodgett (LB) films.[9,10] Much of the work is driven by the application potential of nanoparticles, as an example of which one may consider metal nanoparticles in transparent matrices that are being investigated as non-linear optical materials[11] as well as for third harmonic generation.[12]

In this laboratory, we have developed a technique wherein nanocomposites of colloidal particles in thermally evaporated fatty lipid films can be formed by a simple solution based immersion procedure.[13–16] Attractive electrostatic interactions between charged colloidal particles and oppositely charged amphiphilic molecules in the organic matrix were used to drive the diffusion of the colloidal nanoparticles.[13–16] In a variant of the above process, it is conceivable that alternative and possibly stronger interactions could drive the diffusion of colloidal particles into the organic matrix. One such approach may be based on biomolecular recognition of complementary units such as the well-studied high-affinity ($K_a \sim 10^{15}$ mol^{-1}) specific binding of biotin to avidin/streptavidin.[17,18] The above-mentioned molecular recognition process has been used with success to form multilayer films of avidin and biotin-labeled poly(amine)s,[19] in the organization of ordered networks of superparamagnetic iron oxide nanoparticles,[20] and in the construction of enzyme multilayer films.[21] In this paper, we advance our studies into the formation of nanocomposites using electrostatic interactions to probe the incorporation of avidin protein molecules in thermally evaporated fatty acid films (arachidic acid, AA) and thereafter to assemble biotinylated gold colloidal particles in the fatty acid–avidin composite film *via* the biotin–avidin molecular recognition process. This procedure is illustrated in Scheme 1. In the first step, the fatty acid film is thermally evaporated onto suitable solid supports. The second step consists of immersion of the AA film in the avidin solution until

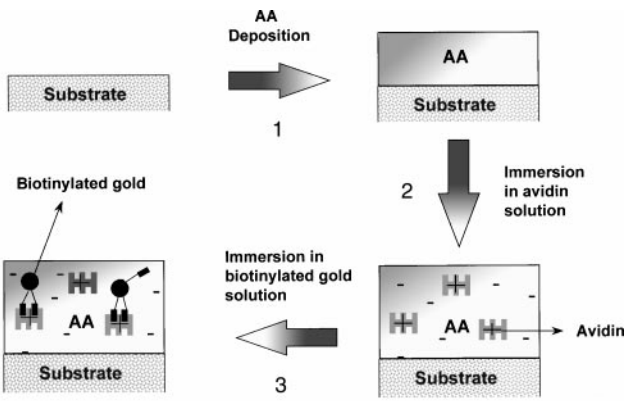

Scheme 1 Diagram illustrating the various stages of formation of nanocomposites of AA. Step 1, deposition of AA films on suitable substrates; step 2, incorporation of avidin molecules in the AA matrix by immersion in protein solution; and step 3, incorporation of biotinylated gold particles in the avidin–AA composite film by immersion in gold colloidal solution. The biotin–avidin molecular recognition process driving nanocomposite formation is illustrated in this step of the procedure.

equilibration of the protein molecule density in the fatty acid matrix is achieved. In the final step, the AA–avidin composite film is immersed in biotinylated gold colloidal particle solution and the colloidal particles assembled in the lipid matrix *via* the biotin–avidin molecular recognition process. The extraction of the protein and gold colloidal particles into the lipid matrix has been studied using quartz crystal microgravimetry (QCM) and UV-vis spectroscopy measurements and analyzed in terms of a one-dimensional diffusion model. The films at various stages of composite formation have been further characterized using Fourier transform infrared (FTIR) spectroscopy. Presented below are details of the investigation.

Experimental details

Aqueous colloidal gold particles were synthesized by citrate reduction of $HAuCl_4$ as described elsewhere.[13] This procedure yielded particles of 130 ± 30 Å size at a pH of *ca.* 3. The gold particles were capped with disulfide biotin as described in an earlier report.[22] Chemisorption of the biotin disulfide molecule on the gold colloidal particle surface *via* a thiolate bond formation with gold leads to biotinylation of the gold particle surface. After biotinylation of the colloidal gold particles, the pH of the solution was adjusted to 8 using buffer solution.

A 10^{-6} M concentrated aqueous solution of avidin (SISCO Research Laboratories) was prepared and the pH adjusted to 3, 8 and 11 using suitable buffer solutions for the immersion measurements.

Thin films of arachidic acid (AA) of *ca.* 1000 Å thickness were thermally evaporated onto gold-coated AT cut quartz crystals (6 MHz frequency), quartz substrates and oxidized Si(111) substrates for QCM, UV-vis and FTIR measurements respectively (step 1, Scheme 1). The AA film depositions were carried out in an Edwards E306A coating unit equipped with a liquid nitrogen trap at a pressure of better that 1×10^{-7} Torr. The film deposition rate and thickness were monitored *in situ* using an Edwards FTM5 QCM. After deposition, the AA films were immersed in the pH 3, 8, 11 avidin solutions and the incorporation of avidin molecules in the fatty acid matrix was followed using QCM, UV-vis and FTIR spectroscopy measurements (step 2, Scheme 1). The QCM measurements were carried out *ex situ* after thorough washing with water and drying of the quartz crystals in flowing N_2. Similar *ex situ* QCM measurements were carried out during immersion of the AA–avidin composite film in biotinylated gold solution at pH 8 after complete diffusion of the protein molecules into the AA matrix was established (step 3, Scheme 1). The frequency measurements were made with the Edwards FTM5 frequency counter which had a stability and resolution of ±1 Hz. For the 6 MHz crystal used, this translates to a mass resolution of 12.1 ng cm^{-2}. The frequency changes measured during incorporation of the avidin molecules as well as the biotinylated gold colloidal particles were converted to mass loading using the standard Sauerbrey formula.[23] It may be mentioned here that QCM measurements of the protein incorporation into separate AA films of 1000 Å thickness at pH 8 (maximum protein incorporation) followed by incorporation of biotinylated gold particles yielded mass uptake values that were within 6–10% of each other in the different runs. This may be taken as a measure of the confidence limits that may be attributed to the QCM measurements of this study.

UV-vis measurements of the AA film on quartz substrates during incorporation of avidin and biotinylated gold colloidal particles were performed on a Hewlett Packard 8542 A diode array spectrophotometer operated at a resolution of 2 nm. FTIR measurements of AA films on Si(111) substrates under similar stages of nanocomposite formation were carried out on a Shimadzu FTIR-8201 PC instrument in the diffuse reflectance mode at a resolution of 4 cm^{-1}.

Results and discussion

Detailed knowledge of the encapsulation of protein molecules in suitable inert hosts is important for the development of biosensors.[24] Proteins have been organized at the surfaces of phospholipids,[25] self-assembled monolayers,[26] in polymer matrices,[27] and by electrostatic attachment to the galleries of α-zirconium phosphate.[28] Avidin protein molecules, which have a pI 10,[29] have amino acid groups on the surface which may be charged by suitable choice of the solution pH. It should be possible, in principle, to extend the method developed by us for the electrostatically controlled diffusion of charged colloidal particles into fatty lipid matrices[13–16] to biologically important molecules such as proteins. Fig. 1 shows a plot of the QCM mass uptake *vs.* time of immersion of a 1000 Å thick AA film in the avidin solution held at pH 8 (circles), while the inset of Fig. 1 shows similar plots of the protein mass uptake recorded during immersion of AA films in pH 3 (triangles) and pH 11 (squares) avidin solutions. The solid lines in Fig. 1 and the inset are based on a 1-D analysis of the QCM data and will be discussed subsequently. It can be seen that, while the kinetics of avidin incorporation in the AA film is rather similar for all the pH solutions up to *ca.* 1000 min of immersion, significant differences are observed between the pH 8 curve and the pH 3 and 11 curves beyond this time interval. The equilibrium protein mass loading for the pH 11 and 3 composite films is nearly identical at 18 and 10 μg cm^{-2} respectively. The concentration of the avidin molecules in the AA matrix stabilizes for these pH values within 2500 min of immersion in the respective solutions. For the film immersed in avidin solution at pH 8, the uptake of avidin is considerably larger and equilibrates at a protein loading of *ca.* 150 μg cm^{-2} in the composite film. This translates into a roughly 700% increase in the protein loading in this film in comparison to the pH 3 and 11 cases. The equilibration of the avidin molecule density in the films takes *ca.* 6000 min at pH 8 and is considerably longer than for the pH 3 and 11 films. A step-like variation in the avidin uptake kinetics with time is clearly observed in the pH 8 mass uptake data (indicated by arrows in Fig. 1) and is similar to the features observed during diffusion of charged colloidal gold and silver particles in fatty amine matrices.[13–16] The variation of the avidin concentration in the films with solution pH may be explained in terms of a simple electrostatic model. At pH 3, while the amino acid

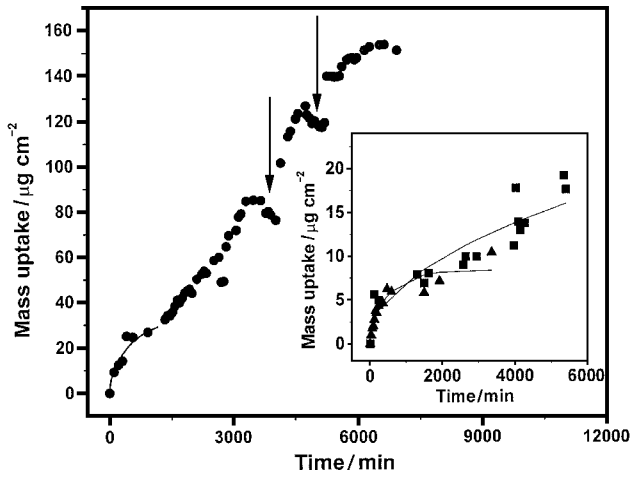

Fig. 1 QCM avidin mass uptake data measured *ex situ* as a function of time of immersion of a 1000 Å thick AA film in 10^{-6} M avidin solution at pH 8. The arrows highlight "steps" in the mass uptake kinetics data. The inset shows the QCM avidin mass uptake data for the AA films immersed in pH 11 (squares) and pH 3 (triangles) protein solutions. The solid lines are based on fits to the QCM data using a 1-D diffusion model (see text for details).

groups on the protein surface would be fully positively charged, the AA molecules in the thermally evaporated film are expected to be fully un-ionized since the pK_a of the acid molecules is *ca.* 5.4.[30] Thus, there would be minimal attractive electrostatic interaction between the fatty acid molecules and the proteins leading to a small number density of avidin molecules in the film. At pH 11, the protein molecules would be close to electrically neutral (pI of avidin = 10) and the AA molecules would be fully negatively charged. This also leads to negligible electrostatic interaction between the host (AA) and guest (avidin) molecules and is reflected in the lower avidin concentration in the film. At pH 8, however, the AA molecules would be fully negatively charged while the avidin molecules would be positively charged. Maximum attractive electrostatic interaction occurs at this pH, leading to enhanced avidin concentration in the film. Thus, electrostatic interactions may be used for the incorporation of protein molecules such as avidin in fatty lipid molecules quite easily by the simple immersion procedure described herein. However, it is important to note that, even in the absence of attractive electrostatic interactions between the protein molecules and the AA host film (at pH 3 and 11), there is considerable avidin uptake in the films, which clearly indicates that additional interactions such as hydrogen bonding, hydrophobic forces *etc.* also play a significant role in driving the proteins into the fatty acid matrix.

The mass loading of *ca.* 150 μg cm^{-2} observed for the AA–avidin composite film grown at pH 8 is extremely large and suggests that surface adsorption of the avidin molecules may also contribute to the protein uptake. It is well known that protein molecules spontaneously concentrate at phase boundaries[31] and therefore we performed contact angle measurements on both the as-deposited AA film as well as the AA–avidin composite film grown at pH 8 on quartz. The contact angle measurements were performed on a sessile water drop (1 μl) using a Rame-Hart 100 goniometer. The contact angles for the AA and the AA–avidin composite films were measured to be 95 and 90° respectively, while the contact angle recorded from an avidin film deposited on quartz by evaporation of a drop of avidin solution was 15°. This clearly indicates that the avidin molecules are entrapped within the hydrophilic regions of the AA matrix as in the case of surface-modified colloidal gold and silver particles[13–16] and adsorption of the avidin molecules on the AA film surface may be ruled out. The large mass uptake may also be a consequence of entrapment of water along with the avidin molecules. We carried out careful measurement of the QCM quartz crystal frequency as a function of drying time of the AA–avidin composite film and observed that frequency stabilization occurred within a time interval of *ca.* 30 min of extraction of the film from solution. Therefore, all QCM mass measurements reported herein have been made after thorough drying (and stabilization of the quartz crystal resonance frequency) of the composite films in N_2 for at least 45 min.

The kinetics of protein incorporation in the AA films studied by QCM measurements (Fig. 1) may be conveniently analyzed in terms of a one-dimensional (1-D) diffusion model as has been demonstrated by us for colloidal nanoparticles of silver, gold and CdS in fatty amine films.[13–16] The mathematical details of the 1-D diffusion model and discussion pertaining to the appropriate boundary conditions in the model may be obtained from refs. 14 and 15 and will not be replicated here. However, we would like to point out that there is considerable swelling of the films during avidin incorporation and therefore the film thickness values used in the 1-D analysis are different from the as-deposited thickness of 1000 Å. The thickness of the composite films after avidin incorporation at different pH values was measured using optical interferometry and are listed in Table 1 along with the values of the avidin concentration at the film/protein solution interface (C_o, molecules cm^{-3}) and the protein diffusivity (D, $Å^2$ min^{-1}). We have not attempted to analyze the protein incorporation profile for the AA–avidin composite film grown at pH 8 beyond 1500 min of immersion due to the "step-like" features observed (Fig. 1) and therefore the values of C_o and D given in Table 1 for this film pertain to analysis of avidin diffusion in the first 1500 min only.

The following observations may be made based on the 1-D analysis results presented in Table 1. The concentration of the avidin molecules at the film/solution interface (C_o) for all pH values is, within a factor of *ca.* 4, nearly identical. The values of C_o are 3–4 orders of magnitude smaller than the nominal protein concentration taken for the experiments and indicates that the interaction of the protein with the lipid matrix does not lead to substantial concentration enhancement at the film surface. In the case of charged colloidal particle diffusion into fatty amine films, we had observed a large enhancement of the particle density at the film/solution interface which was attributed to strong electrostatic interactions between the colloidal particles and the lipid matrix.[13–16] In this respect it appears that the avidin interaction with the AA matrix is considerably weaker and suggests a surface barrier for adsorption. This also underlines the role of interactions other than purely electrostatic which contribute to protein incorporation in the lipid matrix. The protein diffusivities are also seen to be strongly solution pH dependent with maximum diffusivity calculated for the pH 8 case (within the 1500 min diffusion window). The avidin diffusion coefficient is quite large for the pH 3 film and considerably less for the pH 11 film. The large difference in the diffusion coefficients of the protein molecules incorporated at pH 3 and 11 is surprising given that the equilibrium protein mass loading is nearly identical. This aspect along with an apparent surface barrier for protein adsorption at the film/solution interface is not understood at the moment.

From the QCM studies presented above, the optimum conditions for incorporation of avidin molecules in 1000 Å thick AA films is found to be pH 8 and an immersion time of *ca.*

Table 1 Parameters obtained from a 1-D diffusion analysis of QCM mass uptake measurements during extraction of avidin and biotinylated gold particles in AA films

Solution pH	Film thickness/Å	C_o/molecules (clusters) cm^{-3}	D/$Å^2$ min^{-1}
(a) Protein diffusion			
3	2000	3.8×10^{10}	2760
11	2000	1.3×10^{11}	180
8	2000[a]	1.5×10^{11}	2750
(b) Biotinylated gold diffusion			
8	3500[b]	1.5×10^{9}	260

[a] This value is the thickness of the film measured after *ca.* 1500 min of immersion of the 1000 Å thick AA film in avidin solution. [b] This value is the composite film thickness measured after both complete avidin and biotinylated gold particle incorporation.

6000 min. After equilibration of the avidin molecule density in the 1000 Å thick AA film had occurred, the quartz crystal was immersed in biotinylated colloidal gold solution at pH 8 (step 3, Scheme 1) and the mass uptake measured *ex situ* as a function of time of immersion. Fig. 2 shows a plot of the QCM mass uptake with time for the above experiment. It is observed that there is considerable diffusion of the biotinylated colloidal gold particles into the film driven by the avidin–biotin molecular recognition process. This process of colloidal gold incorporation by molecular recognition is shown in step 3 of Scheme 1. The time taken for equilibration of the cluster density in the films to occur is found to be *ca.* 30 000 min (500 h). The equilibrium gold particle density in the film is *ca.* 95 μg cm^{-2} and corresponds to 4.3×10^{12} gold particles cm^{-2} of the film surface. Comparing this density with the equilibrium density of avidin molecules in the film (1.5×10^{15} cm^{-2}) yields a protein/gold colloidal particle ratio of *ca.* 350. Avidin is a tetrameric protein (Scheme 1, step 2) and is capable of binding to four biotin groups simultaneously. The fact that the protein to gold colloidal particle ratio is so high indicates that steric constraints prevent complete coordination of biotin groups on the colloidal particle surface with available sites on the avidin protein surface.

The QCM data of the biotinylated gold particle incorporation in the AA matrix shown in Fig. 2 was also analyzed in terms of a 1-D model and the parameters obtained are listed in Table 1. The mass of the gold particle with the biotin molecules (area per biotin molecule of 25 $Å^2$) was taken to be 20.5×10^{-9} ng for the diffusion analysis. Assuming complete reduction of the gold salt, the gold particle density at the film/solution interface is seen to be *ca.* 2 orders of magnitude less than that of the nominal particle density in the solution (*ca.* 2.8×10^{11} cm^{-3}). This may be a consequence of repulsive electrostatic interaction between the negatively charged citrate reduced gold and the negatively charged AA matrix, which, to some extent, is screened by the positive charges on the avidin molecules in the AA matrix. This is in contrast to the large enhancement of the gold particle concentration observed during electrostatically controlled diffusion into fatty amine films where strong attraction between the particles and film occurs.[16] What is most interesting, however, is the magnitude of the diffusion coefficient calculated for the biotinylated gold particles. The value of 260 $Å^2$ min^{-1} compares quite favorably with the value of 300 $Å^2$ min^{-1} calculated for carboxylated gold particles diffusing into 1000 Å thick octadecylamine films under maximum electrostatic interaction conditions.[16] This indicates that, in spite of the repulsive interaction of the biotinylated colloidal gold particles with the AA matrix, the biotin–avidin high-affinity molecular recognition process is able to drive the diffusion of the gold particles into the matrix quite rapidly and is an important result of this study.

As mentioned above, we have recently carried out a detailed study of the electrostatically controlled diffusion of carboxylic acid derivatized colloidal gold particles of different sizes into thermally evaporated octadecylamine (ODA) films.[16] The equilibrium cluster mass uptake for 130 Å size colloidal gold particles in 1000 Å thick ODA films was found[16] to be 70 μg cm^{-2}. This mass uptake is nearly 25 μg cm^{-2} less than that observed in this study for similar thickness fatty acid films (see Fig. 2). Thus, the avidin–biotin interaction leads not only to a relatively high diffusivity of the colloidal gold particles, but also to a greater colloidal particle density in the composite films than that obtained from purely electrostatic interactions. The strength of the biotin–avidin interaction *vis-à-vis* purely electrostatic interactions appears to play an important role in this process.

The encapsulation of avidin in the AA matrix as well as the subsequent incorporation of biotinylated colloidal gold particles *via* the avidin–biotin molecular recognition process was also studied using UV-vis spectroscopy. These measurements were carried out *ex situ* on a 1000 Å thick AA film on quartz immersed in 10^{-6} M avidin solution at pH 8 (optimum binding conditions for avidin, QCM results above) and thereafter immersed in the biotinylated gold solution (pH 8). Fig. 3 shows plots of the spectra recorded from the AA film under various stages of nanocomposite formation. Curve 1 corresponds to the spectrum recorded from the as-deposited AA film and is essentially featureless in the visible region of the electromagnetic spectrum. After immersion in avidin solution for 150 h, very little change is observed in the visible region and the growth of a resonance at *ca.* 205 nm is seen (curve 2). On immersion of the avidin–AA composite film in the biotinylated solution, interesting changes could be seen in the color of the film with time of immersion and this is reflected in growth of an absorption feature in the UV-vis spectra (curves 3–5, Fig. 3). Curve 3 corresponds to the absorption spectrum recorded from the avidin–AA film after immersion in the gold solution for 100 h while curves 4 and 5 correspond to measurements on the film after immersion for 300 and 500 h respectively. A barely discernible absorption feature at *ca.* 590 nm is seen in curve 3 which clearly grows with time and saturates in intensity after 500 h of immersion (curves 4 and 5).

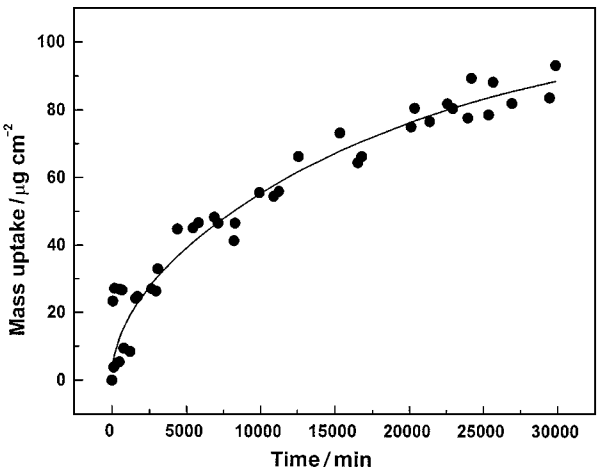

Fig. 2 QCM mass uptake measured *ex situ* as a function of time of immersion of an avidin–AA composite film (thickness 1000 Å) in biotinylated gold solution. The solid line is based on a fit to the QCM data using a 1-D diffusion model (see text for details).

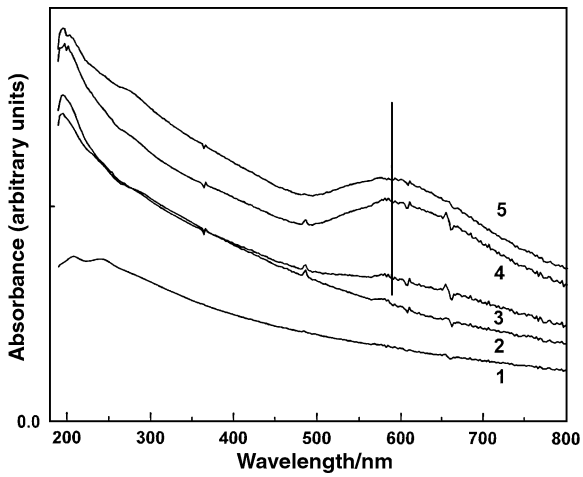

Fig. 3 UV-vis spectra recorded from a 1000 Å thick AA film on quartz during various stages of nanocomposite formation. Curve 1, as-deposited AA film; curve 2, AA film after immersion in 10^{-6} M avidin solution (pH 8) for 150 h; curves 3, 4 and 5, avidin–AA composite film after immersion in biotinylated gold sol for 100, 300 and 500 h respectively. The gold surface plasmon resonance at *ca.* 590 nm is indicated in the figure.

The resonance at *ca.* 590 nm is due to excitation of surface plasmons in the gold particles and is responsible for the striking color of gold colloidal solutions.[32] The growth of the surface plasmon resonance indicates that the biotinylated colloidal gold particle density in the film increases with time and is in agreement with the QCM results presented earlier (Fig. 2). We would like to add here that immersion of the as-deposited AA film directly in the biotinylated gold solution (bypassing step 2, Scheme 1) did not result in a measurable growth of the surface plasmon resonance at 590 nm even after prolonged periods of immersion (500 h). This was cross-checked with QCM measurements as well which yielded negligible mass changes on immersion of the AA film in the gold solution. The above results clearly show that the incorporation of the biotinylated gold particles in the AA film is driven by the high-affinity biotin–avidin interaction. We would like to mention that the plasmon resonance wavelength of *ca.* 590 nm in the films is considerably higher than that recorded from the gold colloidal solution (530 nm)[16] and indicates that the particles are in a close-packed aggregated state in the film. The plasmon resonance wavelength obtained for the biotinylated gold–avidin composites of this study are in agreement with that obtained for gold particle–fatty amine composite films studied earlier.[16]

An important aspect of encapsulation of protein molecules in host structures is ascertaining whether the biological activity of the protein is retained.[28] The host should ideally be inert and not perturb the secondary structure of the protein after incorporation. The secondary structure of proteins is conveniently studied using FTIR spectroscopy measurements.[28,33,34] The amide I and II bands occur at *ca.* 1657 and 1540 cm^{-1} in native proteins and are known to be indicators of the environment in which the proteins are entrapped.[28,33,34] FTIR spectra of a 1000 Å thick AA film on a Si(111) substrate before and after immersion in avidin (10^{-6} M, pH 8) and biotinylated gold solutions (pH 8) for 150 and 500 h, respectively, are shown in Fig. 4. In Fig. 4A, the methylene antisymmetric (2920 cm^{-1}) and symmetric (2850 cm^{-1}) stretch modes are shown for the AA film before (curve 1) and after immersion in avidin (curve 2) and the biotinylated gold solutions (curve 3) as briefly mentioned above. It can be seen that the intensity of the methylene vibrational bands decreases on incorporation of avidin (compare curves 1 and 2) and a further reduction in intensity is observed on incorporation of the biotinylated gold particles. We have observed a similar variation in the intensity of the methylene stretch bands during electrostatic incorporation of surface modified colloidal gold particles in thermally evaporated fatty amine films.[16] This observation has been explained in terms of randomization in the orientation of the hydrocarbon chains as a consequence of incorporation of the nanoparticles in the fatty lipid matrix.[16] Since the avidin molecule is fairly large as are the colloidal gold particles, we believe a similar explanation holds in this case as well. A loss in the AA molecules from the film would also explain this behavior. AA molecules are insoluble in water, and would be expected to separate out at the surface of water and reduce the surface tension of the colloidal solution. However, we have not observed a significant reduction in the surface tension of both avidin and gold colloidal solutions after immersion of the AA films for prolonged periods and it thus appears likely that the reduction in intensity of the methylene stretch bands is due to reorganization in the orientation of the AA hydrocarbon chains.

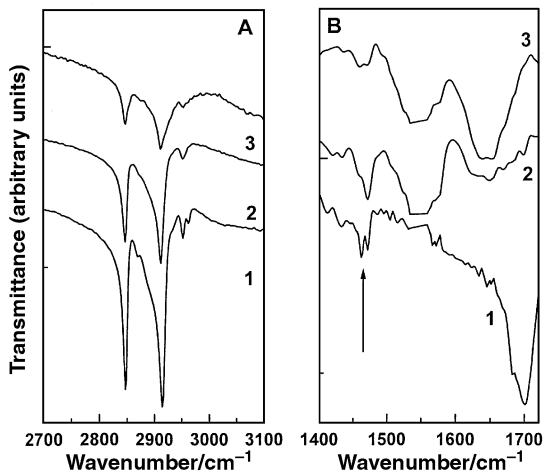

Fig. 4 FTIR spectra of (A) the methylene stretch modes and (B) of the amide I and II bands recorded from a 1000 Å thick AA film on Si(111) during various stages of nanocomposite formation. Curve 1, as-deposited AA film; curve 2, AA film after immersion in 10^{-6} M avidin solution (pH 8) for 150 h; and curve 3, avidin–AA composite film after immersion in biotinylated gold solution for 500 h. The arrow in (B) indicates the methylene scissoring absorption band.

Fig. 4B shows the FTIR spectra recorded for the AA films under similar stages of nanocomposite formation in the spectral range 1400 to 1720 cm^{-1}. Curve 1, which corresponds to the FTIR spectrum recorded from the as-deposited AA film, shows two absorption features at 1700 and *ca.* 1465 cm^{-1} (indicated by an arrow in the figure). The band at 1700 cm^{-1} is due to excitation of carbonyl stretch vibrations and indicates that the matrix is in the un-ionized form.[35,36] The other absorption band is due to excitation of the methylene scissoring mode of vibration and can be clearly seen to be split into two bands at 1474 and 1462 cm^{-1}. The splitting of this band is a clear indication that the hydrocarbon chains in the as-deposited AA matrix are in a microcrystalline environment and in the all-*trans* configuration.[35,36] After equilibration of the avidin molecule density in the film (curve 2), it is seen that the splitting of the methylene scissoring modes is reduced considerably. The intensity of the scissoring band is further reduced on incorporation of biotinylated gold particles in the film (curve 3). This indicates that the hydrocarbon chains are no longer close-packed and suggests considerable reorganization of the chains in the AA matrix. This is in agreement with the FTIR results shown in Fig. 4A where a concomitant reduction in intensity of the methylene stretch vibrations was observed on avidin and biotinylated gold colloidal particle incorporation.

A comparison of curves 1 and 2 in Fig. 4B shows that the carbonyl stretch mode has disappeared on avidin incorporation. It is known for fatty lipid films that salt formation leads to a shift in the carbonyl stretch vibration to around 1540 cm^{-1} (refs. 35 and 36) and a band at this wavelength is observed for the AA–avidin composite film (curve 2). The disappearance of the band at 1700 cm^{-1} indicates fairly strong electrostatic coupling of the avidin molecules with the carboxylate ions of the AA matrix. Unfortunately, the amide II band of the avidin molecule is also known to occur at this wavelength[34] and therefore we are unable to make an unequivocal assignment of the features observed close to 1540 cm^{-1}. The amide I band which is known to occur at 1640 cm^{-1} can be clearly seen in the AA–avidin composite film (curve 2) and indicates that the avidin molecules are incorporated in the AA matrix without significant perturbation to the protein secondary structure. On immersion in the biotinylated gold solution, it is observed that the amide I band increases in intensity and there is a sharpening of the band as well. We are unable to account for this behavior and are currently investigating the avidin–biotin interaction within confined spaces such as those provided by the hydrophilic regions of fatty lipids to understand this better.

To sum up, the FTIR measurements indicate that the avidin molecules are encapsulated within the AA matrix without significant distortion of the protein secondary structure. The

hydrocarbon chains undergo randomization in their orientation as they accommodate the large protein and biotinylated colloidal gold particles. However, the biological activity is mainly dictated by the tertiary structure of the proteins and is not amenable to characterization using FTIR spectroscopy. The fact that the presence of avidin in the AA matrix drives the diffusion of biotinylated gold into the fatty acid film together with the observation that biotinylated gold does not diffuse into the bare AA film clearly shows that the biological activity (and hence the tertiary structure) of avidin (in terms of the biotin–avidin high-affinity binding) is not affected by the encapsulation process.

Conclusions

It has been demonstrated that avidin molecules can be incorporated in thermally evaporated fatty acid films by a simple beaker-based immersion technique. The interaction of the protein molecules with the fatty acid host is predominantly electrostatic. FTIR results show that the protein is encapsulated within the AA matrix without significant perturbation to the protein secondary structure. Biotinylated colloidal gold particles could be incorporated thereafter into the avidin–AA composite film by a similar immersion procedure. The incorporation of colloidal gold particles is driven by the high-affinity biotin–avidin molecular recognition process.

Acknowledgements

NL thanks the Council for Scientific and Industrial Research (CSIR), Government of India, for a research fellowship. The authors acknowledge useful discussions with Dr. Vijaya Patil. This work was funded by a special grant to MS from the CSIR. The biotin disulfide molecule was a gift from Dr. S. P. Chavan, NCL, Pune.

References

1 M. Brust, M. Walker, D. Bethell, D. J. Schiffrin and R. Whyman, *J. Chem. Soc., Chem. Commun.*, 1994, 801.
2 S. Connolly, S. Fullam, B. Korgel and D. Fitzmaurice, *J. Am. Chem. Soc.*, 1998, **120**, 2969.
3 V. L. Colvin, A. N. Goldstein and A. P. Alivisatos, *J. Am. Chem. Soc.*, 1992, **114**, 5221.
4 K. Bandyopadhyay, V. Patil, K. Vijayamohanan and M. Sastry, *Langmuir*, 1997, **13**, 5244.
5 J. H. Fendler and F. C. Meldrum, *Adv. Mater.*, 1995, **7**, 607 and references therein.
6 V. Patil, K. S. Mayya, S. D. Pradhan and M. Sastry, *J. Am. Chem. Soc.*, 1997, **119**, 9281.
7 K. S. Mayya, V. Patil and M. Sastry, *J. Chem. Soc., Faraday Trans.*, 1997, **93**, 3377.
8 K. S. Mayya and M. Sastry, *Langmuir*, 1999, **15**, 1902.
9 C. Zylberaijch-Antoine, A. Barraud, H. Roulet and G. Dufour, *Appl. Surf. Sci.*, 1991, **52**, 323.
10 R. S. Urquhart, D. N. Furlong, H. Mansur, F. Grieser, K. Tanaka and Y. Okahata, *Langmuir*, 1994, **10**, 899.
11 M. Nogami, K. Nagasaka and T. Suzuki, *J. Am. Ceram. Soc.*, 1992, **75**, 220.
12 L. L. Beecroft and C. K. Ober, *Chem. Mater.*, 1997, **9**, 1302.
13 M. Sastry, V. Patil and K. S. Mayya, *Langmuir*, 1997, **13**, 4490.
14 V. Patil and M. Sastry, *J. Chem. Soc., Faraday Trans.*, 1997, **93**, 4347.
15 M. Sastry, V. Patill and S. R. Sainkar, *J. Phys. Chem. B*, 1998, **102**, 1404.
16 V. Patil, R. B. Malvankar and M. Sastry, *Langmuir*, 1999, **15**, 8197.
17 R. Blankenburg, P. Meller, H. Ringsdorf and C. Salesse, *Biochemistry*, 1989, **28**, 8214.
18 J. N. Herron, W. Muller, M. Paudler, H. Riegler, H. Ringsdorf and P. A. Suci, *Langmuir*, 1992, **8**, 1413.
19 J. Anzai, Y. Kobayashi, N. Nakamura, M. Nishimura and T. Hoshi, *Langmuir*, 1999, **15**, 221.
20 M. Li, K. K. W. Wong and S. Mann, *Chem. Mater.*, 1999, **11**, 23.
21 C. Bourdillon, C. Demaille, J. Moiroux and J. M. Saveant, *J. Am. Chem. Soc.*, 1995, **117**, 11499.
22 M. Sastry, N. Lala, V. Patil, S. P. Chavan and A. G. Chittiboyina, *Langmuir*, 1998, **14**, 4138.
23 G. Sauerbrey, *Z. Phys.* (*Munich*), 1959, **155**, 206.
24 S. Braun, S. Rappoport, R. Zusman, S. Shtelzer, S. Druckman, D. Anvir and M. Ottolenghi, in *Biotechnology: Bridging Research and Applications*, ed. D. Kamely, A. Chakrabarty and S. E. Kornguth, Kluwer Academic, Amsterdam, 1991, p. 205.
25 I. Hamachi, A. Fujita and T. Kunitake, *J. Am. Chem. Soc.*, 1994, **116**, 8811.
26 M. Mrkish, G. B. Sigal and G. M. Whitesides, *Langmuir*, 1995, **11**, 4383.
27 B. Miksa and S. Slmokowski, *Colloid Polym. Sci.*, 1995, **273**, 47.
28 C. V. Kumar and G. L. McLendon, *Chem. Mater.*, 1997, **9**, 863.
29 C. E. Jordan and R. M. Corn, *Anal. Chem.*, 1997, **69**, 1449.
30 S. J. Roser and M. R. Lovell, *J. Chem. Soc., Faraday Trans.*, 1995, **91**, 1783.
31 L. Razumovsky and S. Damodaran, *Langmuir*, 1999, **15**, 1392.
32 S. Underwood and P. Mulvaney, *Langmuir*, 1994, **10**, 3427.
33 A. Dong, P. Huang and W. S. Caughey, *Biochemistry*, 1992, **31**, 182.
34 S. Zhao, D. S. Walker and W. M. Reichert, *Langmuir*, 1993, **9**, 3166.
35 P. Ganguly, S. Pal, M. Sastry and M. N. Shashikala, *Langmuir*, 1995, **11**, 1078.
36 J. F. Rabolt, F. C. Burns, N. E. Schlotter and J. D. Swalen, *J. Chem. Phys.*, 1983, **78**, 946.